JCTC Journal of Chemical Theory and Computation

Article

pubs.acs.org/JCTC

Theoretical Study of the Local and Charge-Transfer Excitations in Model Complexes of Pentacene-C_{60} Using Tuned Range-Separated Hybrid Functionals

Cai-Rong Zhang,[†,‡] John S. Sears,[†] Bing Yang,[†,§] Saadullah G. Aziz,[∥] Veaceslav Coropceanu,*[,†] and Jean-Luc Brédas*[,†,∥]

[†]School of Chemistry and Biochemistry and Center for Organic Photonics and Electronics, Georgia Institute of Technology, Atlanta, Georgia 30332-0400, United States

[‡]Department of Applied Physics, Lanzhou University of Technology, Lanzhou, Gansu 730050, P. R. China

[§]State Key Laboratory of Supramolecular Structure and Materials, Jilin University, Changchun, 130012 Jilin, P. R. China

[∥]Department of Chemistry, King Abdulaziz University, Jeddah 21589, Mekkah, Saudi Arabia

Supporting Information

ABSTRACT: The characteristics of the electronic excited states and the charge-transfer processes at organic−organic interfaces play an important role in organic electronic devices. However, charge-transfer excitations have proven challenging to describe with conventional density functional theory (DFT) methodologies due to the local nature of the exchange-correlation potentials often employed. Here, we examine the excited states of model pentacene-C_{60} complexes using time-dependent DFT with, on one hand, one of the most popular standard hybrid functionals (B3LYP) and, on the other hand, several long-range corrected hybrid functionals for which we consider both default and nonempirically tuned range-separation parameters. The DFT results based on the tuned functionals are found to agree well with the available experimental data. The results also underline that the interface geometry of the complex has a strong effect on the energies and ordering of the singlet and triplet charge-transfer states.

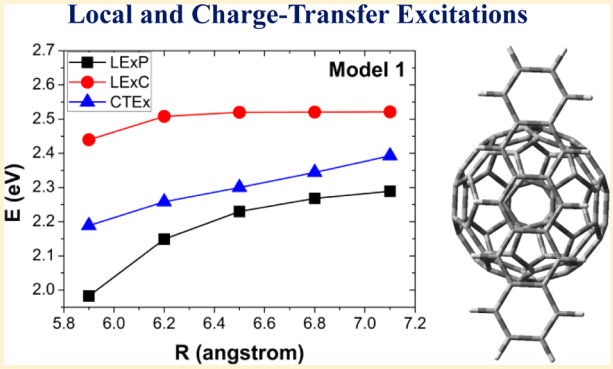

1. INTRODUCTION

The electronic structure at organic−organic interfaces is of great importance in the performance of various organic electronic devices. For instance, the charge-transfer (CT) states at the interface between the electron-donor material and the electron-acceptor material in organic photovoltaic (OPV) cells play a major role in both exciton-dissociation and charge-recombination processes.[1−4] Therefore, obtaining an accurate description of these states is critical to reach a complete understanding of the working principles of OPV devices. A major obstacle in the modeling of CT states arises from the inability of conventional density functional theory (DFT) methods to describe their nature accurately. These difficulties can be traced back to (essentially) two major and interrelated deficiencies of conventional functionals, namely the following: (i) the improper description of the $1/r$ (r = length) dependence for the energy of the CT states at large intermolecular separations due to the local or semilocal nature of the functionals; and (ii) the improper description of the fundamental gaps in molecular systems due to the many-electron self-interaction error (MESIE) that these functionals suffer from. In principle, the inclusion of 100% exact Hartree−Fock (HF) exchange through a hybrid-GGA (generalized gradient approximation) style of approach could provide the proper $1/r$ asymptotic dependence and the cancellation of the one-electron self-interaction. However, in practice, this type of approach does not provide satisfactory results due to the absence of the short-range electron correlation in HF and a delicate balance of the exchange and correlation description in GGA approaches.

The proper description of the asymptotic, $1/r$, dependence can be obtained with recently developed range-separated hybrid (RSH) functionals.[5] In the case of long-range corrected (LRC) functionals, a simple separation of the electron−electron interactions is based upon

$$\frac{1}{r} = \frac{\mathrm{erf}(\omega r)}{r} + \frac{\mathrm{erfc}(\omega r)}{r} \quad (1)$$

where ω corresponds to the range-separation parameter. HF is employed to treat the long-range exchange (in the first term on the right of eq 1), while a local or semilocal DFT functional is

Received: March 26, 2014
Published: April 28, 2014

   dx.doi.org/10.1021/ct500259m | J. Chem. Theory Comput. 2014, 10, 2379−2388

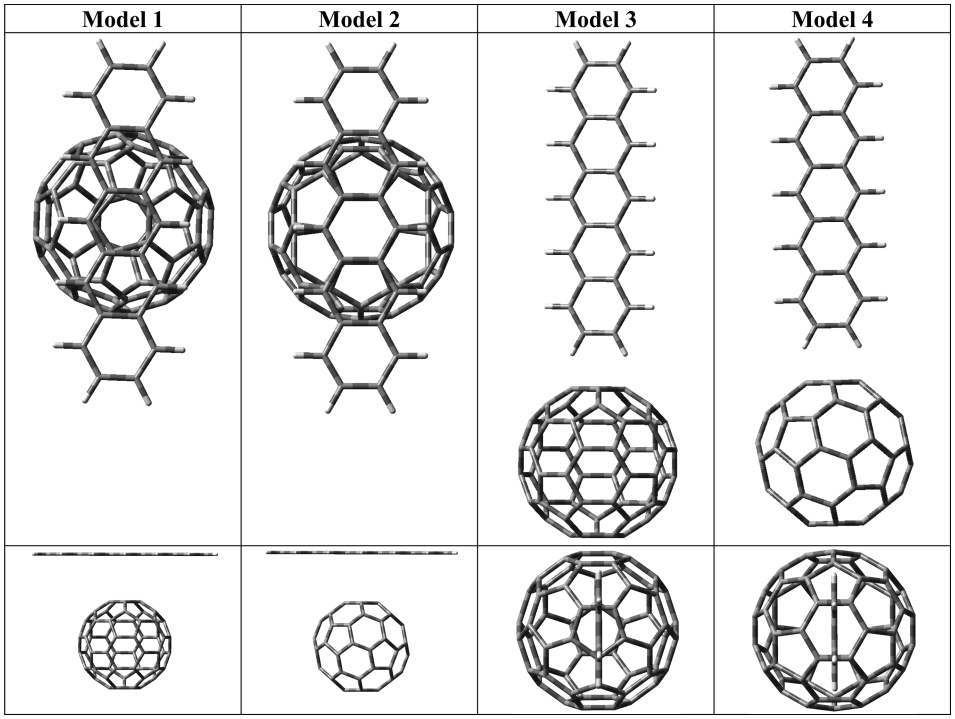

Figure 1. Illustration of the pentacene/C_{60} model systems considered in the work.

used to treat the short-range exchange (in the second term on the right of eq 1). While the inclusion of a complete description of exchange at long-range satisfies the long-range asymptotic dependence of the CT states, the results from these approaches still do not provide satisfactory results (as we show below). The difficulty with usual RSH functionals is that the MESIE gives rise to an error in the HOMO−LUMO gap as compared to the fundamental gap (that corresponds to the difference between the vertical ionization potential (IP) and electron affinity (EA)).[6] These errors can be greater than 1 eV and give rise to an incorrect asymptotic limit even for the RSH functionals. It has been demonstrated that the fundamental gap in molecular systems and solids can be well described with RSH approaches employing a system-dependent range-separation parameter.[7−11] A nonempirical tuning procedure proposed by Stein, Kronik, and Baer for determining the optimal range-separation parameter has paved the way for a quantitative description of the CT states in molecular complexes at the TDDFT level.[12,13] The approach is based upon minimizing the error in describing the fundamental gap of the complex using the Kohn−Sham orbital energies. The tuning procedure that has been used previously[12,14−16] and is employed in this work considers the IP of the donor and the EA of the acceptor through minimizing the following expression

$$J(\omega) = |\varepsilon^{D}_{HOMO} + E^{D}_{gs}(N-1,\omega) - E^{D}_{gs}(N,\omega)| + |\varepsilon^{A}_{HOMO} + E^{A}_{gs}(M,\omega) - E^{D}_{gs}(M+1,\omega)| \quad (2)$$

where the first term in eq 2 is the difference between the HOMO of the donor and the computed IP of the donor and the second term is the difference between the HOMO of the anion and the EA of the acceptor. Optimizing the range-separation parameter to minimize $J(\omega)$ has been shown to provide for a quantitative description of the CT energies in molecular complexes and for cases where the errors from conventional functionals are 1−2 eV.[12] It should be stressed that the tuning in these cases does not involve any empirical data, being self-consistently determined by the system and the specific RSH functional employed.

We note that the description of triplet excitations at the full TDDFT level is problematic for many functionals and especially for the LRC functionals considered here, a result that can be traced back to the wave function instabilities in the ground state.[17,18] While the tuning of the range-separation parameter is expected (as will be shown below) to partially alleviate these problems for many systems, we have also compared the results from TDDFT computations using the Tamm-Dancoff approximation (TDA-TDDFT)[19−21] since this procedure is anticipated to give a more reliable description for the triplet states. We employ below these tuned LRC functionals for the description of the CT states in model pentacene (P)/C_{60} systems.

2. MODEL SYSTEMS

Both bulk and bilayer heterojunctions formed from pentacene as the donor material and C_{60} as acceptor material have been used in OPV devices.[22−25] We have evaluated earlier the impact of the intermolecular geometries on exciton-dissociation and charge-recombination processes for several configurations of the P/C_{60} complexes that are relevant to bilayer and bulk heterojunctions.[26] The local and CT excitation energies of a single P/C_{60} complex were also examined previously by Nakano and co-workers who used RSH functionals with tuned range-separation parameters.[27,28] We note that the latter work was somewhat limited since a single geometric configuration of the P/C_{60} complex was considered, and only the singlet excited states were derived; in addition, a reasonable but somewhat arbitrary intermolecular distance of 3.5 Å was used for the intermolecular separation between pentacene and C_{60}. In order to develop a thorough understanding of the intermolecular CT states in these systems, it is important to consider not only the singlet states but also the triplet

dx.doi.org/10.1021/ct500259m | J. Chem. Theory Comput. 2014, 10, 2379−2388

Table 1. Range-Separation Parameter ω (Given in bohr^{-1}), Orbital Energies, HOMO-LUMO Gap, ΔSCF Triplet Energy ($E_{T1}(\Delta SCF) = E_{T1}^{SCF} - E_{S0}^{SCF}$), and Lowest TDDFT and TDA-TDDFT Excitation Energies to the S_1 and T_1 States of Pentacene[a]

						TDDFT		TDA-TDDFT	
functional	ω	HOMO	LUMO	gap	T_1(ΔSCF)	S_1	T_1	S_1	T_1
LC-BLYP	0.47	−6.73	−0.58	6.15	1.06	2.60	*img*	2.99	0.94
LC-ωPBE	0.40	−6.80	−0.85	5.95	1.02	2.57	*img*	2.92	1.02
ωB97X	0.30	−6.52	−0.70	5.82	1.11	2.49	*img*	2.83	1.12
ωB97XD	0.20	−6.28	−0.90	5.38	1.13	2.37	*img*	2.70	1.11
OPT-LC-BLYP	0.21	−6.05	−0.89	5.16	1.18	2.28	0.71	2.65	1.09
OPT-LC-ωPBE	0.20	−6.17	−1.08	5.09	1.12	2.28	0.52	2.70	1.05
OPT-ωB97X	0.18	−6.03	−0.89	5.14	1.13	2.30	0.40	2.63	1.11
OPT-ωB97XD	0.17	−6.12	−0.98	5.14	1.13	2.31	0.20	2.63	1.10
B3LYP	—	−4.61	−2.40	2.21	1.00	1.95	0.59	2.21	1.10
BLYP	—	−3.88	−2.68	1.20	0.95	1.66	0.84	---	---

[a]*img* stands for an imaginary excitation energy. All energies are given in eV. The experimental values of IP, EA, S_1, and T_1 energies of isolated pentacene are 6.59 eV, 1.39 eV, 2.31, and 0.86 eV, respectively.[52,53,55]

Table 2. Range-Separation Parameter ω (bohr^{-1}), Orbital Energies, HOMO-LUMO Gap, $E_{T1}(\Delta SCF)$, and Lowest TDDFT and TDA-TDDFT Excitation Energies to the S_1 and T_1 States of C_{60}[a]

						TDDFT		TDA-TDDFT	
functional	ω	HOMO	LUMO	gap	T_1(ΔSCF)	S_1	T_1	S_1	T_1
LC-BLYP	0.47	−8.31	−1.48	6.83	3.11	2.92	1.13	3.06	1.95
LC-ωPBE	0.40	−8.43	−1.75	6.68	2.86	2.88	1.14	3.00	2.07
ωB97X	0.30	−8.09	−1.63	6.46	2.98	2.79	1.57	2.86	2.15
ωB97XD	0.20	−7.82	−1.85	5.97	2.53	2.62	1.69	2.68	2.08
OPT-LC-BLYP	0.21	−7.45	−1.74	5.71	2.53	2.50	1.85	2.57	2.02
OPT-LC-ωPBE	0.20	−7.64	−1.99	5.65	2.39	2.48	1.76	2.67	2.02
OPT-ωB97X	0.18	−7.54	−1.83	5.71	2.54	2.52	1.75	2.58	2.05
OPT-ωB97XD	0.17	−7.66	−1.93	5.73	2.54	2.53	1.73	2.59	2.04
B3LYP	—	−5.99	−3.23	2.76	1.90	2.10	1.59	2.10	1.77
BLYP	—	−5.13	−3.42	1.71		1.73	1.52	---	---

[a]All energies are given in eV. The experimental values of IP, EA, S_1, and T_1 energies of C_{60} are 7.69, 2.68, 1.94, and 1.7 eV, respectively.[56−58]

states.[29,30] Furthermore, since the CT energies are sensitive to intermolecular distances and orientations, the investigation of these aspects is also useful.[26,31] Therefore, here, we have examined four different model complexes of P/C_{60} (see Figure 1) in order to investigate the role of molecular orientation on the local (intramolecular) and CT excitation energies. We consider two cofacial, *face-on*, models with the central ring of pentacene centered over either a 5-membered ring (Model 1) or a 6-membered ring (Model 2) of C_{60} as well as two "T-shaped", *edge-on*, complexes with the long axis of the pentacene molecule aligned along the axis connecting the center of C_{60} with either the center of a 5-membered face (Model 3) or a 6-membered face (Model 4). Such model complexes are representative of the structures that are observed at the D/A interfaces;[32,33] therefore, through comparison of the impact of the various configurations, insight can be gained into the role of the detailed structural properties on the electronic states at the interface.

3. THEORETICAL METHODOLOGY

The geometries of pentacene and C_{60} were fully optimized at the DFT level using a 6-31G(d,p) basis set[34,35] and the B3LYP functional.[36,37] B3LYP is known to provide molecular geometries in good comparison to experiment.[38] The B3LYP/6-31G(d,p) molecular geometries were subsequently employed in the construction of the model complexes **1**−**4**. Potential energy surfaces were constructed for each of the model configurations employing both the B3LYP-D[39] and ωB97X-D[40] functionals. Single-point DFT, TDDFT, and TDA-TDDFT calculations were performed for the individual pentacene and C_{60} molecules as well as for the model complexes. Both singlet and triplet excited states were examined. Four LRC functionals have been considered; LC-BLYP,[41,42] LC-ωPBE,[43−46] ωB97X,[47] and ωB97XD; the calculations were carried out with the default as well as the optimally tuned ω values. In addition, for the sake of comparison, we also considered the BLYP and B3LYP functionals. Most single-point DFT, TDDFT, and TDA-TDDFT calculations were performed with the same 6-31G(d,p) basis set employed for the geometry optimizations. The calculations were carried out with the Gaussian 09 package,[48] with exception of the TDA-TDDFT calculations, performed with QChem 3.2.[49] We note that, in the present work, we have not taken into account the surrounding dielectric medium (that would act to stabilize the CT-state energies) since our main goal is the assessment of the performance of optimally tuned LRC functionals.

4. RESULTS AND DISCUSSION

Optimally Tuned Range-Separation Parameters for Pentacene-C_{60}. The optimized ω values for the LC-BLYP, LC-ωPBE, ωB97X, and ωB97XD functionals were obtained by minimizing $J(\omega)$, see eq 2, using separate calculations for the IP and HOMO of pentacene and the EA and LUMO of C_{60} (we considered steps of 0.01 bohr^{-1} in ω). The optimized ω values are 0.21, 0.20, 0.18, and 0.17 bohr^{-1} for LC-BLYP, LC-ωPBE, ωB97X, and ωB97XD, respectively, to be compared to default

dx.doi.org/10.1021/ct500259m | J. Chem. Theory Comput. 2014, 10, 2379−2388

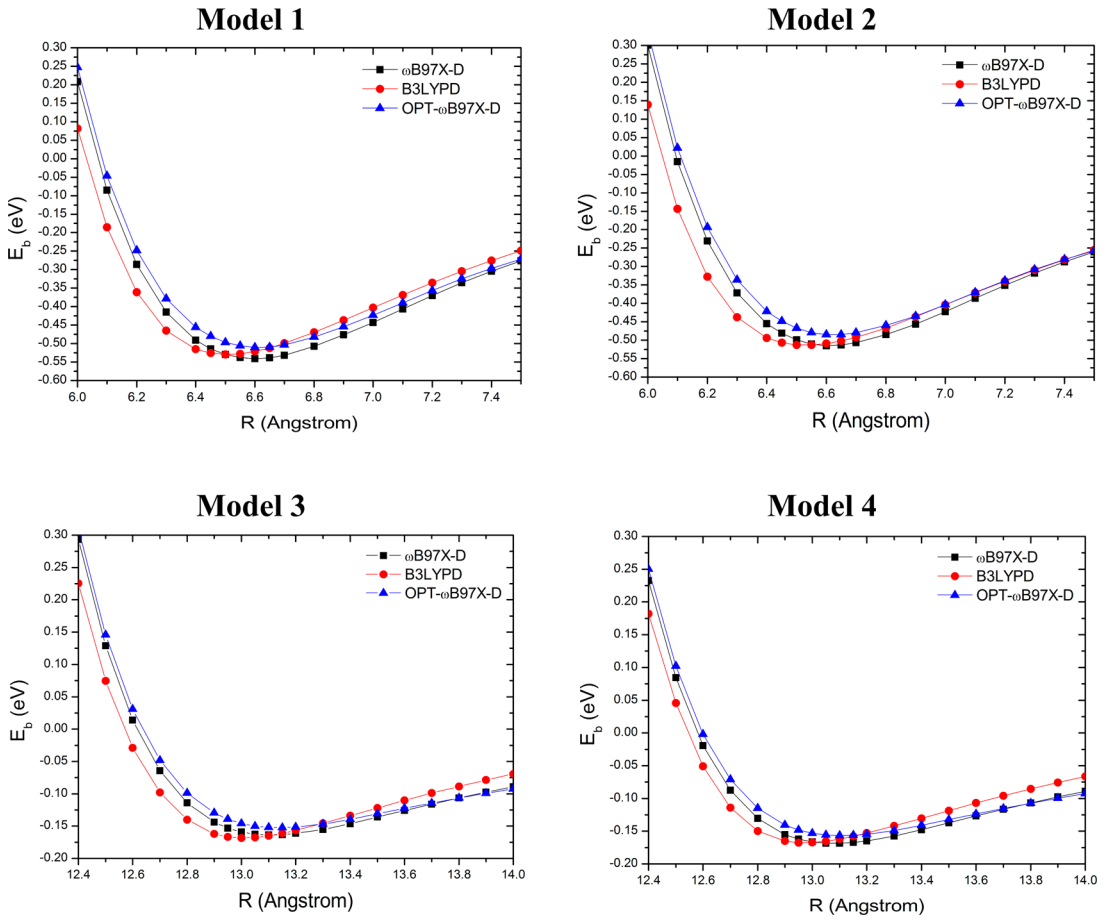

Figure 2. One-dimensional scans of the potential energy surfaces for the four model systems of pentacene-C_{60}.

Table 3. Singlet TDDFT Excitation Energies [eV] in the Face-on Models of Pentacene/C_{60}

model	method	ω	LExP[a]	LExC[b]	CTEx[c]	CTEx-LExP[d]
1	LC-BLYP	0.47	2.55	2.90	3.33	0.78
	LC-ωPBE	0.40	2.52	2.86	3.16	0.64
	ωB97X	0.30	2.44	2.75	3.01	0.57
	ωB97XD	0.20	2.31	2.60	2.48	0.17
	OPT-LC-BLYP	0.21	2.22	2.45	2.33	0.11
	OPT-LC-ωPBE	0.20	2.23	2.47	2.25	0.02
	OPT-ωB97X	0.18	2.23	2.52	2.30	0.07
	OPT-ωB97XD	0.17	2.24	2.53	2.31	0.07
	B3LYP	---	1.90	2.07	1.30	−0.60
2	LC-BLYP	0.47	2.49	2.87	3.30	0.81
	LC-ωPBE	0.40	2.46	2.87	3.17	0.71
	ωB97X	0.30	2.37	2.74	3.02	0.65
	ωB97XD	0.20	2.20	2.60	2.45	0.25
	OPT-LC-BLYP	0.21	2.09	2.45	2.09	0.00
	OPT-LC-ωPBE	0.20	2.06	2.46	2.06	0.00
	OPT-ωB97X	0.18	2.08	2.51	2.08	0.00
	OPT-ωB97XD	0.17	2.09	2.52	2.09	0.00
	B3LYP	---	1.91	2.05	1.20	−0.71

[a]LExP: local excitation in pentacene. [b]LExC: local excitation in C_{60}. [c]CTEx: charge transfer excitation. [d]Difference in energy between the CTEx and LExP states.

Table 4. Singlet TDDFT Excitation Energies [eV] in the Edge-on Models of Pentacene/C_{60}

model	method	ω	LExP[a]	LExC[b]	CTEx[c]	CTEx-LExP[d]
3	LC-BLYP	0.47	2.62	2.91	3.85	1.23
	LC-ωPBE	0.40	2.59	2.88	3.66	1.07
	ωB97X	0.30	2.51	2.79	3.49	0.98
	ωB97XD	0.20	2.38	2.61	3.03	0.65
	OPT-LC-BLYP	0.21	2.29	2.50	2.89	0.60
	OPT-LC-ωPBE	0.20	2.28	2.48	2.77	0.49
	OPT-ωB97X	0.18	2.31	2.52	2.80	0.49
	OPT-ωB97XD	0.17	2.32	2.53	2.80	0.48
	B3LYP	---	1.95	2.09	1.05	−0.90
4	LC-BLYP	0.47	2.62	2.91	3.83	1.21
	LC-ωPBE	0.40	2.59	2.88	3.64	1.05
	ωB97X	0.30	2.51	2.79	3.46	0.95
	ωB97XD	0.20	2.38	2.61	3.00	0.62
	OPT-LC-BLYP	0.21	2.30	2.50	2.86	0.56
	OPT-LC-ωPBE	0.20	2.29	2.48	2.74	0.45
	OPT-ωB97X	0.18	2.31	2.52	2.78	0.47
	OPT-ωB97XD	0.17	2.32	2.53	2.78	0.46
	B3LYP	---	1.96	2.09	1.03	−0.93

[a]LExP: local excitation in pentacene. [b]LExC: local excitation in C_{60}. [c]CTEx: charge transfer excitation. [d]Difference in energy between the CTEx and LExP states.

values for these functionals of 0.47, 0.40, 0.30, and 0.20 $bohr^{-1}$. The notation "OPT-X" used hereafter refers to the results obtained by means of functional X with its optimized ω value. The optimized values for the range-separation parameter are consistent with those observed previously for this[27] as well as similar systems.[12,17,50,51] That the optimized range-separation

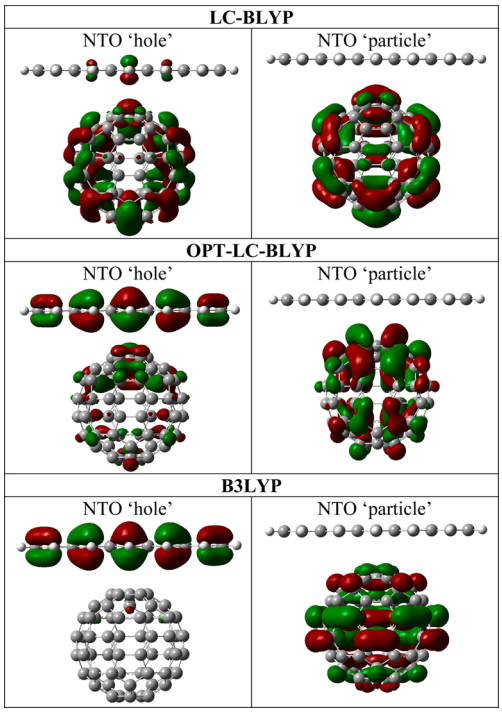

Figure 3. Comparison of the natural transition orbitals for the S_2 state of Model 1 obtained with different functionals.

Table 5. TDDFT Excitation Energies (in eV) for the Pentacene/C_{60} Model Complexes Using Tuned LRC Functionals[a]

		singlet			triplet		
model	method	LExP	LExC	CTEx	LExP	LExC	CTEx
1	OPT-LC-BLYP	2.22	2.45	2.33	0.72	1.85	2.25
	OPT-LC-ωPBE	2.23	2.47	2.25	0.53	1.75	2.20
	OPT-ωB97X	2.23	2.52	2.30	0.42	1.75	2.25
	OPT-ωB97XD	2.24	2.53	2.31	0.25	1.71	2.27
2	OPT-LC-BLYP	2.09	2.45	2.09	0.69	1.82	2.23
	OPT-LC-ωPBE	2.06	2.46	2.06	0.50	1.73	2.17
	OPT-ωB97X	2.08	2.51	2.08	0.38	1.72	2.23
	OPT-ωB97XD	2.09	2.52	2.09	0.18	1.68	2.23
3	OPT-LC-BLYP	2.29	2.50	2.89	0.73	1.85	2.89
	OPT-LC-ωPBE	2.28	2.48	2.77	0.54	1.76	2.77
	OPT-ωB97X	2.31	2.52	2.80	0.43	1.75	2.80
	OPT-ωB97XD	2.32	2.53	2.80	0.25	1.71	2.80
4	OPT-LC-BLYP	2.30	2.50	2.86	0.73	1.85	2.86
	OPT-LC-ωPBE	2.29	2.48	2.74	0.54	1.76	2.74
	OPT-ωB97X	2.31	2.52	2.78	0.43	1.75	2.77
	OPT-ωB97XD	2.32	2.53	2.78	0.33	1.73	2.78

[a]For Model 2, the lowest singlet excited state is a 50:50 mixing of LExP and CTEx, see text, and its energy is given in both corresponding columns.

parameters for ωB97X and ωB97XD are slightly shifted to larger distances with respect to those from LC-BLYP and LC-ωPBE is related to the fixed amount of short-range exchange included in these functionals, an effect that has been observed previously.[17] The optimized ω values vary between 0.21 and 0.17 $bohr^{-1}$, corresponding to a characteristic distance of approximately $1/\omega \sim 5-6$ bohr; thus the separation between the short-range and long-range regions is located at ca. 3 Å, a distance slightly shorter than the separation between the molecules in the P/C_{60} complex.

Table 6. TDA-TDDFT Excitation Energies (in eV) for the Pentacene/C_{60} Model Complexes Using Tuned LRC Functionals

		singlet			triplet		
model	method	LExP	LExC	CTEx	LExP	LExC	CTEx
1	OPT-LC-BLYP	2.60	2.56	2.39	1.09	2.01	2.34
	OPT-LC-ωPBE	2.67	2.66	2.46	1.04	2.01	2.42
	OPT-ωB97X	2.58	2.57	2.31	1.11	2.03	2.29
	OPT-ωB97XD	2.59	2.58	2.32	1.10	2.02	2.30
2	OPT-LC-BLYP	2.71	2.55	2.29	1.07	1.99	2.28
	OPT-LC-ωPBE	2.77	2.64	2.33	1.02	1.99	2.35
	OPT-ωB97X	2.67	2.55	2.20	1.08	2.00	2.25
	OPT-ωB97XD	2.68	2.56	2.21	1.08	2.00	2.26
3	OPT-LC-BLYP	2.66	2.57	2.96	1.10	2.02	2.96
	OPT-LC-ωPBE	2.71	2.67	2.97	1.06	2.02	2.97
	OPT-ωB97X	2.63	2.57	2.80	1.12	2.04	2.80
	OPT-ωB97XD	2.64	2.59	2.80	1.12	2.04	2.80
4	OPT-LC-BLYP	2.66	2.57	2.93	1.10	2.02	2.93
	OPT-LC-ωPBE	2.71	2.67	2.94	1.06	2.02	2.94
	OPT-ωB97X	2.63	2.57	2.78	1.12	2.04	2.78
	OPT-ωB97XD	2.64	2.59	2.78	1.12	2.04	2.78

Local (Molecular) States. Before turning to a discussion of the complexes, it is worth discussing the important differences observed in the computed molecular properties for pentacene and C_{60}. The computed HOMO and LUMO energies, the TDDFT and TDA-TDDFT transition energies for both the S_1 and T_1 states, and the ΔSCF triplet energies are reported in Table 1 for pentacene and Table 2 for C_{60}. At the SCF level, all functionals employed predict the proper closed-shell singlet ground states for both systems. However, the results from the LRC functionals with default range-separation values exhibit a restricted Kohn−Sham to unrestricted Kohn−Sham (RKS-UKS) instability for pentacene, meaning that there is a lower-energy spin-contaminated UKS singlet state solution. As we have discussed previously,[17] this has serious repercussions for the description of the excited states at the TDDFT level.

The experimental IP and EA of pentacene are 6.59 eV[52] and 1.39 eV,[53] respectively, giving a fundamental gap of 5.20 eV. Reliable theoretical estimates of the vertical IP and EA have been obtained with the GW approximation, giving a vertical IP (VIP) of 6.12 eV and a gap of 4.76 eV.[54] The value for $\in_{HOMO}$ for BLYP differs from the experimental IP and the GW VIP by more than 2 eV. This discrepancy is only slightly alleviated with a hybrid-GGA functional (approximately by the percentage of included HF exchange); it remains 1.92 eV away from the experimental estimates when using the popular B3LYP functional. A similar trend is observed in the EAs, with BLYP and B3LYP yielding 2.68 and 2.40 eV, respectively, more than 1 eV larger than the experimental EA. The fundamental gaps from BLYP and B3LYP are thus underestimated for pentacene by as much as 3−4 eV when compared to the difference of the experimental IP and EA or in comparison to the gap from GW. The default-ω LRC and tuned LRC functionals provide in all cases significant improvements in comparison to the experimental IP, EA, and gap values with the errors reduced to less than 1 eV. The LRC functionals with the default range-separation parameter provide values close to the experimental IP of pentacene, while the tuned LRC functionals all provide values remarkably close to the 6.12 eV obtained for the VIP

dx.doi.org/10.1021/ct500259m | J. Chem. Theory Comput. 2014, 10, 2379−2388

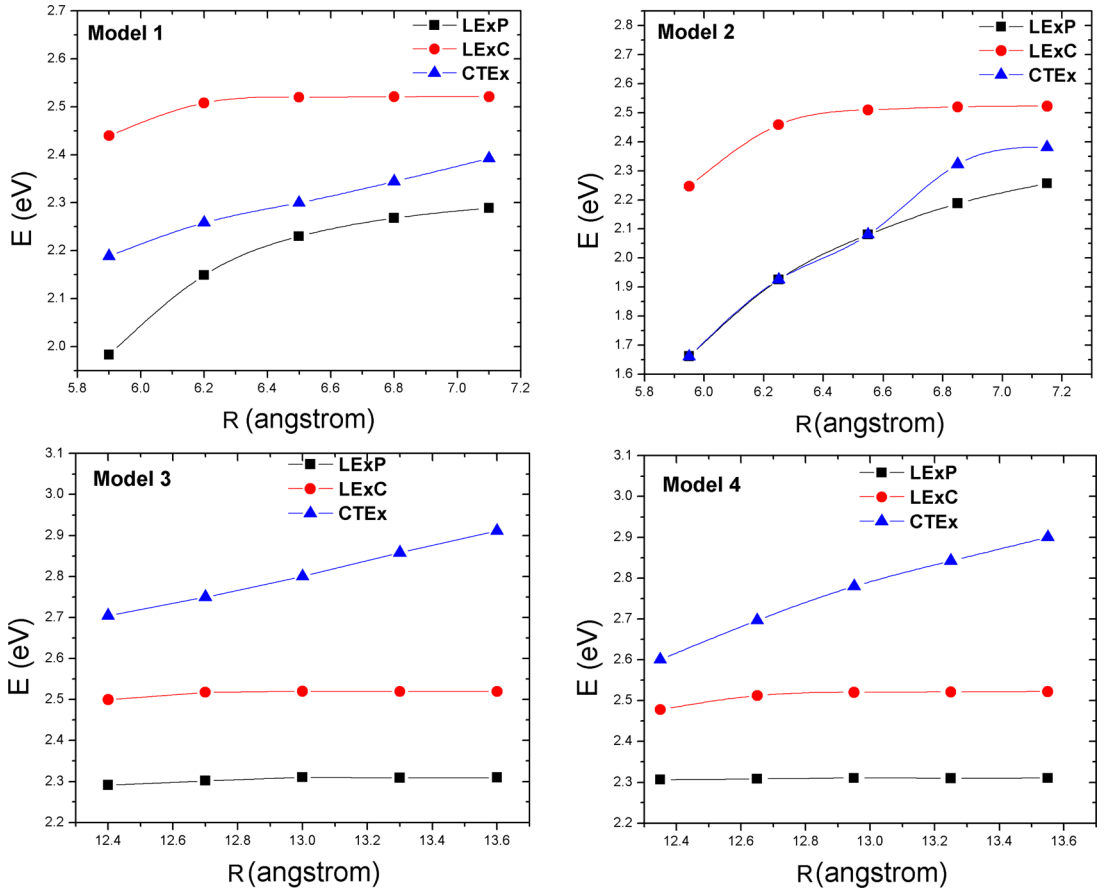

Figure 4. Dependence of the local and CT states on center-to-center intermolecular distance.

with GW. The tuned functionals provide for an improved description of the EA for pentacene in comparison to those with the default range-separation parameter, resulting in gaps that are within ~0.1 eV of the experimental gap and only a few tenths of an eV from the GW results.

The experimental IP and EA of C_{60} are 7.69 and 2.68 eV, respectively,[56] giving a fundamental gap of 5.01 eV. The GW results predict a VIP of 7.41 eV and a slightly smaller gap of 4.91 eV in comparison to experiment.[54] As was observed for pentacene, the gap from BLYP is greatly underestimated (by ~3.4 eV); again this error is reduced in B3LYP by a magnitude approximately proportional to the amount of included exchange (20% in this case). The gaps from the default-ω LRC functionals are all overestimated, with the agreement greatly improving upon tuning the range-separation parameters. We recall, see eq 2, that the range separation parameters are tuned to balance the description of both pentacene and C_{60}. An improved description of C_{60} could no doubt be obtained with a different choice of ω[50] but at the expense of the description of pentacene. Overall, the results for the IP, EA, and fundamental gaps in pentacene and C_{60} paint a clear picture that the LRC functionals provide an improved description of the frontier energies as compared to the popular GGA and hybrid-GGA approaches; further improvements in this description are obtained through the optimization of the range-separation parameter.

The experimental energy of the pentacene first singlet excited state (S_1) is 2.10 eV in solution,[59] 1.85 eV in the solid state,[60,61] and 2.31 eV in the gas phase.[55] The fluorescence spectra for isolated C_{60} suggest that the origin of the $S_0 \rightarrow S_1$ transition is about 1.94 eV;[57] in the solid state, this value reduces to about 1.7 eV.[58] BLYP underestimates the energy of S_1 in both systems, while B3LYP underestimates it for pentacene and agrees reasonably well with the experimental result for C_{60}. Without tuning of the range-separation parameter, the LRC functionals significantly overestimate the $S_0 \rightarrow S_1$ transition for both molecules. Upon tuning, the description is improved for both systems, with excellent agreement with the experimental results for pentacene and a moderate overestimation of the $S_0 \rightarrow S_1$ transition in C_{60}. The energy of the T_1 state can be assessed based either upon the difference of the SCF ground-state energies for the singlet and triplet or through TDDFT calculations. Experimentally, the triplet state in pentacene is about 0.86 eV above the ground state,[62] while for C_{60} it is estimated to be at about 1.55 eV.[57] The ΔSCF triplet energy for both systems is overestimated by as much as a few tenths of an eV in comparison to the experimental results. At the TDDFT level, the triplet energy for pentacene is very poorly described with the default range-separation parameters; indeed, all default-ω LRC functionals predict complex-valued roots to the TDDFT equations, an effect that can be traced back to instabilities in the ground-state wave function for these functionals.[17] The tuning removes this deficiency and the performance for the triplet energy is comparable to that of B3LYP with errors on the order of a few tenths of an eV. B3LYP provides excellent agreement with the experimental triplet energies of C_{60} at the TDDFT level, while the errors from the LRC functionals remain a few tenths of an eV. The TDA-TDDFT triplet energies are not sensitive to ω; they are

dx.doi.org/10.1021/ct500259m | J. Chem. Theory Comput. 2014, 10, 2379−2388

superior to those from full TDDFT for pentacene but inferior in the case of C_{60}.

Overall, by providing a balanced description of the molecular properties (IP, EA, S_1, and T_1 energies), the tuned range-separated functionals are thus found to provide a superior description of the electronic structure of pentacene and C_{60}. Of particular importance in this regard is the improved description of the IP and EA values by the HOMO and LUMO energies, which has implications for the descriptions of the CT states in the P/C_{60} complexes. Among the tuned LRC functionals none of the functionals is seen to outperform the others for this particular case as the results never differ by more than ∼0.2 eV for any of the molecular properties computed.

Ground-State Potential Energy Surface of the Pentacene/C_{60} Complexes. The energies of the CT states and the extent of their mixing with the local excitations either in pentacene or C_{60} are sensitive to the relative orientations of the molecules (especially the donor−acceptor distance given the $1/r$ dependence) and will be impacted by the detailed geometric structure at the organic−organic interface. Due to the importance of weak dispersion interactions in determining the configurations of such systems, these geometries can often be difficult to describe at the DFT level. Empirical dispersion corrections to the DFT energies provide at present an efficient approach to incorporate these effects at reasonable computational expense. We have conducted one-dimensional scans of the ground-state potential energy surface (PES) of the P/C_{60} complex using a frozen-monomer approach and employing three functionals incorporating an empirical treatment of dispersion, namely B3LYP-D, ωB97X-D, and OPT-ωB97X-D.[63] The PESs from each of these functionals are presented in Figure 2.

The magnitudes of the binding energies for the face-on models (Model 1 and Model 2) are approximately three times as large as for those of the edge-on models (Model 3 and Model 4). The binding energies are in the range of 0.51−0.54 eV for Model 1 and of 0.49−0.52 eV for Model 2. The molecular center-to-center distances range between 6.5 and 6.6 Å in both models, with the B3LYP-D geometries being slightly more compact than those with the LRC functionals. This gives face-on π-stacking distances between the central ring of pentacene and the nearest ring of C_{60} between 3.2 and 3.4 Å. In the edge-on complexes, with binding energies ∼0.16 eV (about six times the room temperature thermal energy), the center-to-center distances are ∼13 Å in all cases, giving an equilibrium distance of approximately 2.7 Å between the center of the closest ring on C_{60} and the nearest hydrogens of pentacene. Again, the B3LYP-D geometries tend to be somewhat more compact and with slightly larger binding energies than what is found with the other functionals. In any event, the three functionals provide very similar descriptions of the equilibrium distances and the binding energies of pentacene-C_{60}. When constructing the model complexes, the center-to-center distances are fixed at 6.50, 6.55, 13.00, and 12.95 Å for Models 1, 2, 3, and 4, respectively, as derived from the B3LYP-D calculations.

Singlet States of the Model Complexes. The lowest singlet excitation energies for both local and CT excitations are presented in Tables 3 and 4. For all model systems, the TD-B3LYP calculations predict the lowest singlet excited state to be essentially a pure charge-transfer state located about 0.5−1.0 eV below the pentacene S_1. In fact, the first several excited singlet states are predicted to be CT states at the B3LYP level. When turning to LRC functionals, the CT states are blue-shifted by more than 1 eV in energy. The energy of the CT state varies significantly among the default LRC functionals and increases substantially with an increase in the ω value. For example, in Model 3, the excited-state energy grows from 3.03 eV with ωB97X-D to 3.85 eV with LC-BLYP. The tuning of the range-separation parameter brings the results from all LRC functionals into close agreement; the differences among estimated local and CT excitation energies are never more than ∼0.1 eV.

For edge-on Models 3 and 4, the local excitation energies in pentacene (LExP) and in C_{60} (LExC) calculated with different functionals are very close to the corresponding values for the isolated pentacene and C_{60} molecules. For instance for Model 3, the excitation energies of 2.29 and 2.50 eV calculated by means of the OPT-LC-BLYP functional for LExP and LExC, respectively, deviate from those obtained for the isolated molecules by less than 0.01 eV. These results confirm the weak interaction between pentacene and C_{60} for edge-on molecular interfaces. The CT states for Models 3 and 4 derived by means of OPT-LRC functionals are located about 0.25−0.40 eV above the first excited state of C_{60} and about 0.45−0.60 eV above the first excited state of pentacene.

In the face-on models, due to strong intermolecular π−π interactions, there occurs a significant hybridization between the pentacene and C_{60} molecular orbitals. As a consequence, the lowest CT state is substantially lowered in energy in comparison to the edge-on models and mixes with local states. In the case of Model 1, the first CT state, i.e. the S_2 state, is located between the first excited states of pentacene and C_{60}. As can be seen from Figure 3, the natural transition orbitals (NTO) derived for S_2 indicates that while being predominantly a CT state it has also some admixture of C_{60} component. We note that the results from default-ω LRC functionals indicate that depending on the value of ω the lowest CT state could be located above or below the first excited state of C_{60}. Importantly, in the case of Model 2, which is the configuration that due to symmetry reasons allows for the largest π−π interaction, the CT state is further pushed to lower energies and now strongly mixes with the local state on pentacene. In fact, for the intermolecular distance considered here, the TDDFT results (see Figure S1 in the SI) indicate that the first excited state of the complex represents a 50:50 mixture of the local S_1 of pentacene and of a CT component due to electron transfer from the pentacene HOMO to the C_{60} LUMO. An important consequence of the energy lowering related to this mixing is that this lowest singlet excited state of Model 2 with substantial CT character lies *below* the lowest CT triplet state, *vide infra*.

Triplet States of the Model Complexes. Comparisons of the triplet and singlet CT energies derived by means of TD-DFT and TDA-TDDFT calculations using tuned LRC functionals (see the SI for all results) are given in Tables 5 and 6. As in the case of the singlet states, the LRC calculations with optimized ω values predict very similar energies for the triplet CT states. The triplet energies and their dependence on P/C_{60} geometry obtained with the TD-DFT and TDA-TDDFT methods also compare very well.

The results indicate that the local triplet states have energies similar to those in the isolated molecules, which suggests that the local triplet excitations in P/C_{60} are not very sensitive to intermolecular interactions. The situation is different for the CT triplet states, the energies of which strongly depend on

system configuration. The CT triplets in face-on complexes are located about 0.5 eV below those in edge-on complexes. In the case of the edge-on structures, the energies of the lowest singlet and triplet CT states are identical. This degeneracy is, however, lifted in the case of face-on structures. Interestingly, in the case of Model 1, the first CT triplet state lies slightly below the CT singlet state, while, in the case of Model 2, the situation is reversed (due to the strong mixing between the singlet CT state and the local pentacene singlet excited state, as discussed above). These results suggest that the singlet−triplet splitting of the CT states can be controlled by the fine details of the intermolecular orientations. We also note that the switch in the relative positions of the triplet and singlet CT states could have a major effect on charge-recombination processes.[1,30]

The Impact of Intermolecular Distance. Finally, we investigated the dependence of the local and CT singlet state energies on the intermolecular distance. The results are displayed in Figure 4. As expected, for edge-on Models 3 and 4, the increase in intermolecular distance has only a minor effect on the local states. For the range of intermolecular distances considered here, the CT excitation energies in these two models increase nearly in a linear fashion with the increase in intermolecular distance. In the face-on Models 1 and 2, due to stronger intermolecular interactions, both CT and local excitation energies are sensitive to the intermolecular distance; while for large intermolecular distances the excitation energies of both pentacene and C_{60} states converge to the corresponding values of the isolated molecules, the convergence for pentacene occurs at a slower pace. The most interesting situation occurs in Model 2 where the first excited state of pentacene is strongly mixed with the first CT state. As the intermolecular distance increases (and intermolecular interactions decreases) the first excited state of the complex regains the pentacene character, while the second excited state now corresponds to the first CT state, exactly as in the case of Model 1.

4. CONCLUSIONS

In this work, the energetics of pentacene/C_{60} complexes with four different geometrical configurations were investigated by means of LRC functionals. The local and CT states of the complexes were evaluated by means of the TDDFT and TDA-TDDFT approaches. The calculations show that the local excitation energies agree well with the available experimental results.

In the case of default-ω LRC functionals, the CT energies are calculated to strongly depend on the choice of the functional. Upon tuning the range-separation parameter, all LRC functionals considered here give comparable results for both local and CT states. Importantly, our study also indicates that the interface geometry has a strong effect on the following: (i) the CT energies, which are consistent with the large widths of the CT bands observed experimentally,[2] and (ii) the relative positions of the lowest CT triplet and singlet states, which should have a significant impact on charge-recombination and charge-regeneration processes.

■ ASSOCIATED CONTENT

Supporting Information

Triplet excitation energies obtained with default-ω LRC functionals; plots of the frontier molecular orbitals relevant for the description of the lowest CT state; and Cartesian coordinates of the model complexes investigated. This material is available free of charge via the Internet at http://pubs.acs.org.

■ AUTHOR INFORMATION

Corresponding Authors

*E-mail: coropceanu@gatech.edu.

*E-mail: jean-luc.bredas@chemistry.gatech.edu.

Notes

The authors declare no competing financial interest.

■ ACKNOWLEDGMENTS

The work at Georgia Tech was supported by the Deanship of Scientific Research (DSR), King Abdulaziz University, Jeddah, Saudi Arabia, under International Collaboration Grant No. D-001-433 and by the Office of Naval Research under Grant No. N000141410171. C.R.Z. and B.Y. thank the Chinese Visiting Scholar Program sponsored by the China Scholarship Council for support of their stay at Georgia Tech. C.R.Z. also thanks the National Natural Science Foundation of China (Grant No. 11164016) for financial support. The authors are grateful to Dr. Thomas Koerzdoerfer for stimulating discussions.

■ REFERENCES

(1) Bredas, J. L.; Norton, J. E.; Cornil, J.; Coropceanu, V. Molecular Understanding of Organic Solar Cells: The Challenges. *Acc. Chem. Res.* **2009**, *42*, 1691−1699.

(2) Vandewal, K.; Albrecht, S.; Hoke, E. T.; Graham, K. R.; Widmer, J.; Douglas, J. D.; Schubert, M.; Mateker, W. R.; Bloking, J. T.; Burkhard, G. F.; Sellinger, A.; Frechet, J. M. J.; Amassian, A.; Riede, M. K.; McGehee, M. D.; Neher, D.; Salleo, A. Efficient Charge Generation by Relaxed Charge-Transfer States at Organic Interfaces. *Nat. Mater.* **2014**, *13*, 63−68.

(3) Gelinas, S.; Rao, A.; Kumar, A.; Smith, S. L.; Chin, A. W.; Clark, J.; van der Poll, T. S.; Bazan, G. C.; Friend, R. H. Ultrafast Long-Range Charge Separation in Organic Semiconductor Photovoltaic Diodes. *Science* **2014**, *343*, 512−516.

(4) Beljonne, D.; Cornil, J.; Muccioli, L.; Zannoni, C.; Bredas, J. L.; Castet, F. Electronic Processes at Organic-Organic Interfaces: Insight from Modeling and Implications for Opto-Electronic Devices. *Chem. Mater.* **2011**, *23*, 591−609.

(5) Leininger, T.; Stoll, H.; Werner, H. J.; Savin, A. Combining Long-Range Configuration Interaction with Short-Range Density Functionals. *Chem. Phys. Lett.* **1997**, *275*, 151−160.

(6) Bredas, J. L. Mind the Gap. *Mater. Horiz.* **2014**, *1*, 17−19.

(7) Stein, T.; Eisenberg, H.; Kronik, L.; Baer, R. Fundamental Gaps in Finite Systems from Eigenvalues of a Generalized Kohn-Sham Method. *Phys. Rev. Lett.* **2010**, *105*, 266802.

(8) Salzner, U.; Baer, R. Koopmans' Springs to Life. *J. Chem. Phys.* **2009**, *131*, 231101.

(9) Eisenberg, H. R.; Baer, R. A New Generalized Kohn-Sham Method for Fundamental Band-Gaps in Solids. *Phys. Chem. Chem. Phys.* **2009**, *11*, 4674−4680.

(10) Livshits, E.; Baer, R. A Well-Tempered Density Functional Theory of Electrons in Molecules. *Phys. Chem. Chem. Phys.* **2007**, *9*, 2932−2941.

(11) Refaely-Abramson, S.; Sharifzadeh, S.; Jain, M.; Baer, R.; Neaton, J. B.; Kronik, L. Gap Renormalization of Molecular Crystals from Density-Functional Theory. *Phys. Rev. B* **2013**, *88*, 081204.

(12) Stein, T.; Kronik, L.; Baer, R. Reliable Prediction of Charge Transfer Excitations in Molecular Complexes Using Time-Dependent Density Functional Theory. *J. Am. Chem. Soc.* **2009**, *131*, 2818−2820.

(13) Stein, T.; Kronik, L.; Baer, R. Prediction of Charge-Transfer Excitations in Coumarin-Based Dyes Using a Range-Separated Functional Tuned from First Principles. *J. Chem. Phys.* **2009**, *131*, 244119.

(14) Karolewski, A.; Stein, T.; Baer, R.; Kümmel, S. Communication: Tailoring the Optical Gap in Light-Harvesting Molecules. *J. Chem. Phys.* **2011**, *134*, 151101.

(15) Garza, A.; Osman, O.; Wazzan, N.; Khan, S.; Asiri, A.; Scuseria, G. A Computational Study of the Nonlinear Optical Properties of Carbazole Derivatives: Theory Refines Experiment. *Theor. Chem. Acc.* **2014**, *133*, 1−8.
(16) Pandey, L.; Doiron, C.; Sears, J. S.; Bredas, J.-L. Lowest Excited States and Optical Absorption Spectra of Donor-Acceptor Copolymers for Organic Photovoltaics: A New Picture Emerging from Tuned Long-Range Corrected Density Functionals. *Phys. Chem. Chem. Phys.* **2012**, *14*, 14243−14248.
(17) Sears, J. S.; Koerzdoerfer, T.; Zhang, C.-R.; Bredas, J.-L. Orbital Instabilities and Triplet States from Time-Dependent Density Functional Theory and Long-Range Corrected Functionals. *J. Chem. Phys.* **2011**, *135*, 151103.
(18) Peach, M. J. G.; Williamson, M. J.; Tozer, D. J. Influence of Triplet Instabilities in Tddft. *J. Chem. Theory Comput.* **2011**, *7*, 3578−3585.
(19) Wang, Y. L.; Wu, G. S. Improving the Tddft Calculation of Low-Lying Excited States for Polycyclic Aromatic Hydrocarbons Using the Tamm-Dancoff Approximation. *Int. J. Quantum Chem.* **2008**, *108*, 430−439.
(20) Hsu, C. P.; Hirata, S.; Head-Gordon, M. Excitation Energies from Time-Dependent Density Functional Theory for Linear Polyene Oligomers: Butadiene to Decapentaene. *J. Phys. Chem. A* **2001**, *105*, 451−458.
(21) Hirata, S.; Head-Gordon, M. Time-Dependent Density Functional Theory within the Tamm-Dancoff Approximation. *Chem. Phys. Lett.* **1999**, *314*, 291−299.
(22) Yoo, S.; Domercq, B.; Kippelen, B. Efficient Thin-Film Organic Solar Cells Based on Pentacene/C-60 Heterojunctions. *Appl. Phys. Lett.* **2004**, *85*, 5427−5429.
(23) Yoo, S.; Potscavage, W. J.; Domercq, B.; Han, S. H.; Li, T. D.; Jones, S. C.; Szoszkiewicz, R.; Levi, D.; Riedo, E.; Marder, S. R.; Kippelen, B. Analysis of Improved Photovoltaic Properties of Pentacene/C_{60} Organic Solar Cells: Effects of Exciton Blocking Layer Thickness and Thermal Annealing. *Solid-State Electron.* **2007**, *51*, 1367−1375.
(24) Cheyns, D.; Gommans, H.; Odijk, M.; Poortmans, J.; Heremans, P. Stacked Organic Solar Cells Based on Pentacene and C_{60}. *Sol. Energy Mater.* **2007**, *91*, 399−404.
(25) Sullivan, P.; Jones, T. S. Pentacene/Fullerene (C_{60}) Heterojunction Solar Cells: Device Performance and Degradation Mechanisms. *Org. Electron.* **2008**, *9*, 656−660.
(26) Yi, Y. P.; Coropceanu, V.; Bredas, J. L. Exciton-Dissociation and Charge-Recombination Processes in Pentacene/C_{60} Solar Cells: Theoretical Insight into the Impact of Interface Geometry. *J. Am. Chem. Soc.* **2009**, *131*, 15777−15783.
(27) Minami, T.; Nakano, M.; Castet, F. Nonempirically Tuned Long-Range Corrected Density Functional Theory Study on Local and Charge-Transfer Excitation Energies in a Pentacene/C60 Model Complex. *J. Phys. Chem. Lett.* **2011**, *2*, 1725−1730.
(28) Minami, T.; Ito, S.; Nakano, M. Functional Dependence of Excitation Energy for Pentacene/C_{60} Model Complex in the Nonempirically Tuned Long-Range Corrected Density Functional Theory. *Int. J. Quantum Chem.* **2013**, *113*, 252−256.
(29) Johnson, J. C.; Nozik, A. J.; Michl, J. High Triplet Yield from Singlet Fission in a Thin Film of 1,3-Diphenylisobenzofuran. *J. Am. Chem. Soc.* **2010**, *132*, 16302−16303.
(30) Rao, A.; Chow, P. C. Y.; Gelinas, S.; Schlenker, C. W.; Li, C. Z.; Yip, H. L.; Jen, A. K. Y.; Ginger, D. S.; Friend, R. H. The Role of Spin in the Kinetic Control of Recombination in Organic Photovoltaics. *Nature* **2013**, *500*, 435−439.
(31) Sini, G.; Sears, J. S.; Bredas, J. L. Evaluating the Performance of Dft Functionals in Assessing the Interaction Energy and Ground-State Charge Transfer of Donor/Acceptor Complexes: Tetrathiafulvalene-Tetracyanoquinodimethane (Ttf-Tcnq) as a Model Case. *J. Chem. Theory Comput.* **2011**, *7*, 602−609.
(32) Breuer, T.; Witte, G. Diffusion-Controlled Growth of Molecular Heterostructures: Fabrication of Two-, One-, and Zero-Dimensional C_{60} Nanostructures on Pentacene Substrates. *ACS Appl. Mater. Interfaces* **2013**, *5*, 9740−9745.
(33) Rand, B. P.; Cheyns, D.; Vasseur, K.; Giebink, N. C.; Mothy, S.; Yi, Y. P.; Coropceanu, V.; Beljonne, D.; Cornil, J.; Bredas, J. L.; Genoe, J. The Impact of Molecular Orientation on the Photovoltaic Properties of a Phthalocyanine/Fullerene Heterojunction. *Adv. Funct. Mater.* **2012**, *22*, 2987−2995.
(34) Francl, M. M.; Pietro, W. J.; Hehre, W. J.; Binkley, J. S.; Gordon, M. S.; Defrees, D. J.; Pople, J. A. Self-Consistent Molecular-Orbital Methods. 23. A Polarization-Type Basis Set for 2nd-Row Elements. *J. Chem. Phys.* **1982**, *77*, 3654−3665.
(35) Krishnan, R.; Binkley, J. S.; Seeger, R.; Pople, J. A. Self-Consistent Molecular-Orbital Methods 0.20. Basis Set for Correlated Wave-Functions. *J. Chem. Phys.* **1980**, *72*, 650−654.
(36) Becke, A. D. Density-Functional Thermochemistry. 3. The Role of Exact Exchange. *J. Chem. Phys.* **1993**, *98*, 5648−5652.
(37) Lee, C. T.; Yang, W. T.; Parr, R. G. Development of the Colle-Salvetti Correlation-Energy Formula into a Functional of the Electron-Density. *Phys. Rev. B* **1988**, *37*, 785−789.
(38) Sousa, S. F.; Fernandes, P. A.; Ramos, M. J. General Performance of Density Functionals. *J. Phys. Chem. A* **2007**, *111*, 10439−10452.
(39) Antony, J.; Grimme, S. Density Functional Theory Including Dispersion Corrections for Intermolecular Interactions in a Large Benchmark Set of Biologically Relevant Molecules. *Phys. Chem. Chem. Phys.* **2006**, *8*, 5287−5293.
(40) Chai, J. D.; Head-Gordon, M. Long-Range Corrected Hybrid Density Functionals with Damped Atom-Atom Dispersion Corrections. *Phys. Chem. Chem. Phys.* **2008**, *10*, 6615−6620.
(41) Becke, A. D. Density-Functional Exchange-Energy Approximation with Correct Asymptotic-Behavior. *Phys. Rev. A* **1988**, *38*, 3098−3100.
(42) Iikura, H.; Tsuneda, T.; Yanai, T.; Hirao, K. A Long-Range Correction Scheme for Generalized-Gradient-Approximation Exchange Functionals. *J. Chem. Phys.* **2001**, *115*, 3540−3544.
(43) Tawada, Y.; Tsuneda, T.; Yanagisawa, S.; Yanai, T.; Hirao, K. A Long-Range-Corrected Time-Dependent Density Functional Theory. *J. Chem. Phys.* **2004**, *120*, 8425−8433.
(44) Vydrov, O. A.; Heyd, J.; Krukau, A. V.; Scuseria, G. E. Importance of Short-Range Versus Long-Range Hartree-Fock Exchange for the Performance of Hybrid Density Functionals. *J. Chem. Phys.* **2006**, *125*, 074106.
(45) Vydrov, O. A.; Scuseria, G. E. Assessment of a Long-Range Corrected Hybrid Functional. *J. Chem. Phys.* **2006**, *125*, 234109.
(46) Vydrov, O. A.; Scuseria, G. E.; Perdew, J. P. Tests of Functionals for Systems with Fractional Electron Number. *J. Chem. Phys.* **2007**, *126*, 154109.
(47) Chai, J. D.; Head-Gordon, M. Systematic Optimization of Long-Range Corrected Hybrid Density Functionals. *J. Chem. Phys.* **2008**, *128*, 084106.
(48) Frisch, M. J.; Trucks, G. W.; Schlegel, H. B.; Scuseria, G. E.; Robb, M. A.; Cheeseman, J. R.; Scalmani, G.; Barone, V.; Mennucci, B.; Petersson, G. A.; Nakatsuji, H.; Caricato, M.; Li, X.; Hratchian, H. P.; Lzmaylov, A. F.; Bloino, J.; Zheng, G.; Sonnenberg, J. L.; Hada, M.; Ehara, M.; Toyota, K.; Fukuda, R.; Hasegawa, J.; Ishida, M.; Nakajima, T.; Honda, Y.; Kitao, O.; Nakai, H.; Vreven, T.; Montgomery, J. A., Jr.; Peralta, J. E.; Ogliaro, F.; Bearpark, M.; Heyd, J. J.; Brothers, E.; Kudin, K. N.; Staroverov, V. N.; Keith, T.; Kobayashi, R.; Normand, J.; Raghavachari, K.; Rendell, A.; Burant, J. C.; Lyengar, S. S.; Tomasi, J.; Cossi, M.; Rega, N.; Millam, J. M.; Klene, M.; Knox, J. E.; Cross, J. B.; Bakken, V.; Adamo, C.; Jaramillo, J.; Gomperts, R.; Stratmann, R. E.; Yazyev, O.; Austin, A. J.; Cammi, R.; Pomelli, C.; Ochterski, J. W.; Martin, R. L.; Morokuma, K.; Zakrzewski, V. G.; Voth, G. A.; Salvador, P.; Dannenberg, J. J.; Dapprich, S.; Daniels, A. D.; Farkas, O.; Foresman, J. B.; Ortiz, J. V.; Cioslowski, J.; Fox, D. J. *Gaussian 09*, Revision B.01; Gaussian, Inc.: Wallingford, CT, 2009.
(49) Shao, Y.; Molnar, L. F.; Jung, Y.; Kussmann, J.; Ochsenfeld, C.; Brown, S. T.; Gilbert, A. T. B.; Slipchenko, L. V.; Levchenko, S. V.; O'Neill, D. P.; DiStasio, R. A.; Lochan, R. C.; Wang, T.; Beran, G. J.

O.; Besley, N. A.; Herbert, J. M.; Lin, C. Y.; Van Voorhis, T.; Chien, S. H.; Sodt, A.; Steele, R. P.; Rassolov, V. A.; Maslen, P. E.; Korambath, P. P.; Adamson, R. D.; Austin, B.; Baker, J.; Byrd, E. F. C.; Dachsel, H.; Doerksen, R. J.; Dreuw, A.; Dunietz, B. D.; Dutoi, A. D.; Furlani, T. R.; Gwaltney, S. R.; Heyden, A.; Hirata, S.; Hsu, C. P.; Kedziora, G.; Khalliulin, R. Z.; Klunzinger, P.; Lee, A. M.; Lee, M. S.; Liang, W.; Lotan, I.; Nair, N.; Peters, B.; Proynov, E. I.; Pieniazek, P. A.; Rhee, Y. M.; Ritchie, J.; Rosta, E.; Sherrill, C. D.; Simmonett, A. C.; Subotnik, J. E.; Woodcock, H. L.; Zhang, W.; Bell, A. T.; Chakraborty, A. K.; Chipman, D. M.; Keil, F. J.; Warshel, A.; Hehre, W. J.; Schaefer, H. F.; Kong, J.; Krylov, A. I.; Gill, P. M. W.; Head-Gordon, M. Advances in Methods and Algorithms in a Modern Quantum Chemistry Program Package. *Phys. Chem. Chem. Phys.* **2006**, *8*, 3172−3191.

(50) Refaely-Abramson, S.; Baer, R.; Kronik, L. Fundamental and Excitation Gaps in Molecules of Relevance for Organic Photovoltaics from an Optimally Tuned Range-Separated Hybrid Functional. *Phys. Rev. B* **2011**, *8*, 075144.

(51) Isaacs, E. B.; Sharifzadeh, S.; Ma, B.; Neaton, J. B. Relating Trends in First-Principles Electronic Structure and Open-Circuit Voltage in Organic Photovoltaics. *J. Phys. Chem. Lett.* **2011**, *2*, 2531−2537.

(52) Gruhn, N. E.; da Silva Filho, D. A.; Bill, T. G.; Malagoli, M.; Coropceanu, V.; Kahn, A.; Bredas, J. L. The Vibrational Reorganization Energy in Pentacene: Molecular Influences on Charge Transport. *J. Am. Chem. Soc.* **2002**, *124*, 7918−7919.

(53) Crocker, L.; Wang, T.; Kebarle, P. Electron Affinities of Some Polycyclic Aromatic Hydrocarbons, Obtained from Electron-Transfer Equilibria. *J. Am. Chem. Soc.* **1993**, *115*, 7818−7822.

(54) Blase, X.; Attaccalite, C.; Olevano, V. First-Principles Gw Calculations for Fullerenes, Porphyrins, Phtalocyanine, and Other Molecules of Interest for Organic Photovoltaic Applications. *Phys. Rev. B* **2011**, *83*, 115103.

(55) Heinecke, E.; Hartmann, D.; Muller, R.; Hese, A. Laser Spectroscopy of Free Pentacene Molecules (I): The Rotational Structure of the Vibrationless S_1 <- S_0 Transition. *J. Chem. Phys.* **1998**, *109*, 906−911.

(56) Wang, X. B.; Woo, H. K.; Wang, L. S. Vibrational Cooling in a Cold Ion Trap: Vibrationally Resolved Photoelectron Spectroscopy of Cold C_{60} Anions. *J. Chem. Phys.* **2005**, *123*, 051106.

(57) Orlandi, G.; Negri, F. Electronic States and Transitions in C-60 and C-70 Fullerenes. *Photochem. Photobiol. Sci.* **2002**, *1*, 289−308.

(58) Akimoto, I.; Ashida, M.; Kan'no, K. Luminescence from C-60 Single Crystals in Glassy Phase under Site-Selective Excitation. *Chem. Phys. Lett.* **1998**, *292*, 561−566.

(59) Sakamoto, Y.; Suzuki, T.; Kobayashi, M.; Gao, Y.; Fukai, Y.; Inoue, Y.; Sato, F.; Tokito, S. Perfluoropentacene: High-Performance P-N Junctions and Complementary Circuits with Pentacene. *J. Am. Chem. Soc.* **2004**, *126*, 8138−8140.

(60) Faltermeier, D.; Gompf, B.; Dressel, M.; Tripathi, A. K.; Pflaum, J. Optical Properties of Pentacene Thin Films and Single Crystals. *Phys. Rev. B* **2006**, *74*, 125416.

(61) Jundt, C.; Klein, G.; Sipp, B.; Lemoigne, J.; Joucla, M.; Villaeys, A. A. Exciton Dynamics in Pentacene Thin-Films Studied by Pump-Probe Spectroscopy. *Chem. Phys. Lett.* **1995**, *241*, 84−88.

(62) Burgos, J.; Pope, M.; Swenberg, C. E.; Alfano, R. R. Heterofission in Pentacene-Doped Tetracene Single-Crystals. *Phys. Status Solidi B* **1977**, *83*, 249−256.

(63) Agrawal, P.; Tkatchenko, A.; Kronik, L. Pair-Wise and Many-Body Dispersive Interactions Coupled to an Optimally Tuned Range-Separated Hybrid Functional. *J. Chem. Theory Comput.* **2013**, *9*, 3473−3478.